JOURNAL OF ENERGY IN SOUTHERN AFRICA

Determination of oxidation characteristics and decomposition kinetics of some Nigerian biomass

EC Okoroigwe,[a,b,*] SO Enibe,[b] SO Onyegegbu[b]

a. National Centre for Energy Research and Development, University of Nigeria, 1 University Road, Nsukka 410001, Nigeria

b. Department of Mechanical Engineering, University of Nigeria, 1 University Road, Nsukka 410001, Nigeria

Abstract

The oxidation characteristics and devolatilisation kinetics studies of palm kernel shell (Elaeis guineensis), African bush mango wood and shell (Irvingia wombolu), and African border tree wood (Newbouldia laevis), were carried out by the thermogravimetric method. A thermogravimetric analyser TA Q500 instrument was used at a heating rate of 30 °C.min^{-1} under oxidative conditions. It was observed that all the samples followed a two-stage structural decomposition between 200 °C and 500 °C. The greatest mass loss rate occurred within the oxidation stage (200–375 °C) in all the samples. The ignition temperature of the samples ranged from 275–293 °C while their burnout temperatures ranged from 475–500 °C. During the oxidation stage, African bush mango shell was the most reactive sample, while palm kernel shell was the least. During the char combustion stage (375–500 °C), the reactivity of palm kernel shell was the highest. The average activation energy of the samples for the entire decomposition period are 140, 270, 131 and 231 kJ.mol^{-1} respectively. The biomass samples considered are thus suitable for combustion purposes for bioenergy production with minimal external energy input.

Keywords: thermogravimetric analysis; combustion index; activation energy; biomass; bioenergy reaction order

Journal of Energy in Southern Africa 27(3): 39–49

Corresponding author:
Tel. +234-8057156223, email: edmund.okoroigwe@unn.edu.ng

1. Introduction

The prevailing issues of fossil fuels as primary energy sources have continued to provoke interest in exploiting suitable biomass resources for combustion processes in the energy industry. Climate change persistence, environmental pollution and degradation, uneven widespread of fossil deposit, and price fluctuations are among the problems which integrating biomass into the primary energy production has aimed to abate. With biofuel recognised as an alternative fuel source that is net carbon dioxide-neutral, policies to integrate it into national energy mixes have been promoted by some governments. For instance, Nigeria's biofuel policy stipulated a blend of up to 10% ethanol with gasoline, even though the biofuel would be imported for the initial three years until capacity and capability (infrastructure) are built for local production (Anyaoku, 2007). The policy envisages the country achieve a 100% biofuel production by 2020. Brazil's biofuel programme has a long history (Soccol *et* al., 2005), with the fuel contributing to local fuel consumption and export. Germany is the largest producer of biodiesel, with Argentina, Brazil, France, Italy, Malaysia and the USA as other leading producers and consumers of biodiesel (Ubrabio & Getulio, 2010). South Africa's national biofuel strategic policy targeted a 2% biofuel integration into the liquid fuel mix by 2015 (DME, 2007).

As the policies are implemented globally at different scales, biomass demand for energy production is going to increase in the near future. In order to forestall the challenge of inadequate supply of suitable plant varieties, a good number of possible biomass species need to be screened for their potential for bioenergy production. As a contribution to this, some biomass species in Nigeria such as palm kernel shell (Elaeis guineensis), African bush mango wood and shell (Irvingia gabonensis/wombolu), and African border tree wood (Newbouldia laevis), were selected for determination of their combustion properties. Palm kernel shell (PKS) is a common residue from oil palm produce which is rich in carbon and is commercially produced in Nigeria and neighbouring West African countries. About 5–7% of a typical fresh palm fruit bunch is composed of PKS, suggesting its relative abundance (Okoroigwe & Saffron, 2012). Similarly, African bush mango (locally called Ogbono) wood and its shell are common residues in the growing and processing of the seed kernel and pulp (for the sweet species), which are commonly consumed as food in West and Central Africa. They are among some highly valuable and extensively utilised tropical African trees (Ainge & Brown, 2001). After extraction of the seed, the shell is generally dumped at waste collection sites. The tree is classified as a non-timber tree even though it attains a height of up to 30 m and a girth of about 1.0 m when fully developed (Extension bulletin, 1999). According to Ayuk *et* al. (1999), about 169 kg per grower of Irvingia spp seed is recorded in three divisions in Cameroon. Usually, the shell of Irvirngia spp is about five times the mass of the kernel (seed), which would amount to about 845 kg of shell produced per grower in the divisions. The African border tree (called Ogirisi in South-Eastern Nigeria) is non-edible, but medicinal values of its leaves and bark have been reported (Okpala, 2015; Bafor & Sanni, 2009; Ejele *et* al., 2012), and it is commonly used as a land boundary marker. It is a fast-growing, soft-wood and drought-resistant tree.

Thermogravimetric (TG) analysis is the most commonly applied thermoanalytical technique in solid-phase thermal degradation studies (Ninan, 1989) for the purposes of understanding and establishing their thermal degradation kinetics. Usually, the mass of the material heated at a specific heating rate is monitored with respect to time and temperature. Some researchers have used the technique to study the thermal decomposition of biomass under oxidative and inert conditions. For instance, Wilson *et* al. (2011) studied the thermal degradation characteristics of bagasse, palm stem, cashew nut shells, coffee husks, and sisal bole under oxidative conditions, and found that cashew nut shells were the most reactive of the samples, based on their mass loss rate and lower burnout temperature. Similarly, Munir *et* al. (2009) used the TG method to establish the combustion kinetics of cotton stalk, sugar cane bagasse and shea meal, while El may *et* al. (2012) characterised date palm residue using TG analysis under oxidative conditions.

Understanding the decomposition kinetics and combustion behaviour of the selected biomass would aid in the design of chemical processes leading to biofuel production from them. This is in agreement with similar understanding derived from studies of the kinetics of thermal decomposition of other fuels such as coal char (Roberts *et* al., 2015; Niu *et* al., 2016), plastics (Apaydin-Varol *et* al., 2014), municipal solid waste (Conesa & Rey, 2015) and biodiesel (Lin *et* al., 2013). Hence, the objective of this investigation is to determine the combustion and decomposition characteristics of the four tropical biomass species using the TG method. The plants are classified as agricultural residues, non-tree timber and wild plant (non-food plant). The residues constitute environmental nuisance if they are not burnt to dispose of them. In large-scale plantations, their offcuts (residues), pose problems for agricultural machines; there is therefore a need to find an alternative use for the residues.

2. Material and method

2.1 Feedstock

In this investigation, four biomass samples, viz: palm kernel shell (*Elaeis guineensis*), African bush

mango wood and its shell (*Irvingia* gabonensis/wombolu), and the African border tree wood (*Newbouldia laevis*), were randomly selected for the study. The woody samples are counted as non-timber trees even though they can grow large trunks. The feedstock samples obtained within Nsukka town in South East, Nigeria, were air dried and milled to particles of about 1 mm using a Wiley milling machine. TGA was used to determine the devolatilisation data for plotting the TG and the derivative thermogravimetric (DTG) curves. The sample masses used were 24.989 mg, 14.284 mg, 18.840 mg, and 14.907 mg for PKS, African bush mango (ABM) wood, African bush mango (ABM) shell and African border tree (ABT) wood respectively while thermogravimetric analyser, model TGA Q500 was used in the temperature range of 30–750 °C under synthetic air at a temperature gradient of 30 °C.min^{-1}.

2.2 Kinetic study

Kinetic parameters of biomass materials such as activation energy, reaction order and pre-exponential (frequency) factor can be determined by many models. Several investigations have used the Arrhenius equation for the determination of the parameters in both oxidative and inert conditions because of its flexibility and simplicity, compared with other models (Munir et al., 2009; El may et al., 2012; Sait et al., 2012; Parthasarathy et al., 2013; Jeguirim et al., 2014). The Arrhenius model is used in this investigation in determining activation energy, reaction order and frequency factors that governed the decomposition of the feedstock in oxidative conditions. All models used for biomass kinetic studies are based on rate laws that obey Arrhenius rate expression in Equation 1:

$$K(T) = Ae^{-E/RT} \quad (1)$$

where k(T) is temperature dependent reaction rate constant, A is pre-exponential or frequency factor, E is activation energy (J.mol^{-1}), R is the universal gas constant – 8.314 J.mol.$^{-1}$K^{-1}, and T is absolute temperature, K.

The activation energy is regarded as 'the energy threshold that must be overcome before molecules can get close enough to react and form products' (White et al., 2011).

The kinetics of biomass decomposition can be expressed by the relation in Equation 2.

$$\frac{D\alpha}{Dt} = k(T)f(\alpha) = Ae^{-E/RT}\, f(\alpha) \quad (2)$$

where t is time, α is degree of conversion, dα/dt is rate of isothermal process, and f(α) is the conversion function that represents the model used which depends on the controlling mechanism, according to Equation 3.

$$f(\alpha) = (1-\alpha)^n \quad (3)$$

By definition, α can be expressed as the mass fraction of biomass substrate that has decomposed in a time t during the decomposition process or mass fraction of volatiles evolved as shown in Equation 4 (White et al., 2011).

$$\alpha = \frac{m_o - m}{m_o - m_f} \quad (4)$$

where m_o, is the mass of the biomass substrate at the beginning of reaction or initial time, m is the mass of the biomass substrate at any time t, and m_f, is the mass of the biomass at the end of the reaction time. The unreacted mass or residue is accounted for in m_f.

For non-isothermal decomposition, the rate expression which represents reaction rates as function of temperature at a linear heating rate is given in Equation 5.

$$\frac{d\alpha}{dT} = \frac{d\alpha}{dt}\frac{dt}{dT} = \frac{A}{\gamma}e^{-E/RT}\, f(\alpha) \quad (5)$$

where $\frac{d\alpha}{dT}$ is the non-isothermal reaction rate, $\frac{d\alpha}{dt}$ is the isothermal reaction rate and $\frac{dt}{dT}$ is the reciprocal of heating rate (γ^{-1}).

There are many methods to solve Equation 5. The Coats-Redfern (1964) method is the popular non-isothermal model fitting method used for the determination of the reaction processes (Shen et al., 2009).

Integral of both sides of Equation 5 results in the general solution given in Equation 6.

$$g(\alpha) = \int_0^\alpha \frac{d(\alpha)}{f(\alpha)} = \frac{A}{\gamma}\int_{T_0}^{T} \exp(-\frac{E}{RT})dT \quad (6)$$

Using Rainveil's (1960) approximation, the right hand side of Equation 6 can be approximated to Equation 7.

$$g(\alpha) = \frac{ART^2}{\gamma E}\left[1 - \frac{2RT}{E}\right]e^{-\frac{E}{RT}} \quad (7)$$

Further simplification of the rate Equation 7 results in the linear relationship between the reaction rate and temperature given in Equation 8.

$$ln\left[\frac{g(\alpha)}{T^2}\right] = ln\left[\frac{AR}{\gamma E}\left(1 - \frac{2RT}{E}\right)\right] - \frac{E}{RT} \quad (8)$$

The term 2RT/E is usually small, however, hence the linear correlation between the kinetic parameters can be obtained by Equation 9.

$$ln\left[\frac{g(\alpha)}{T^2}\right] = ln\left[\frac{AR}{\gamma E}\right] - \frac{E}{RT} \quad (9)$$

The plot of logarithmic rate of reaction, $\left[\frac{g(\alpha)}{T^2}\right]$, against reciprocal of temperature, T^{-1}, is a straight line whose slope and intercept are –E/R and $ln\left[\frac{AR}{\gamma E}\right]$ respectively. From these, activation energy E, reaction order n and frequency factor A can be estimated.

2.3 Combustion parameters

2.3.1 Reactivity

The reactivity of the biomass samples under oxidative condition was determined according to the method defined by Munir *et* al. (2009), El may *et* al. (2012), Park & Jang (2012) and Ghetti *et* al. (1996). The DTG curve height is a measure of the reactivity of the samples during decomposition stage, hence reactivity R_M is directly proportional to the maximum weight loss rate R_{DTGmax} and inversely proportional to its corresponding peak temperature T_{Peak}. This is given in Equation 10.

$$R_M = 100 \sum \frac{R_{DTGmax}}{T_{DTGmax}} \quad (10)$$

The summation takes account of any secondary peak or shoulder present in each of the regions considered.

2.3.2 Ignition and burn-out temperature

The ignition temperature T_i is the temperature at which major decomposition of the biomass samples began to take place. It is determined by the method described by Xiang-guo *et* al. (2006) according to Figure 1 using the TG and DTG plots of each sample. From the maximum DTG point A, in the oxidation stage, a line is drawn to touch the TG curve at point B. From this point a line BC is drawn as tangent to point B to meet an extended TG level line at C. From point C a vertical line is drawn to touch the temperature scale at point D. The value indicated by D is the approximate ignition temperature T_i.

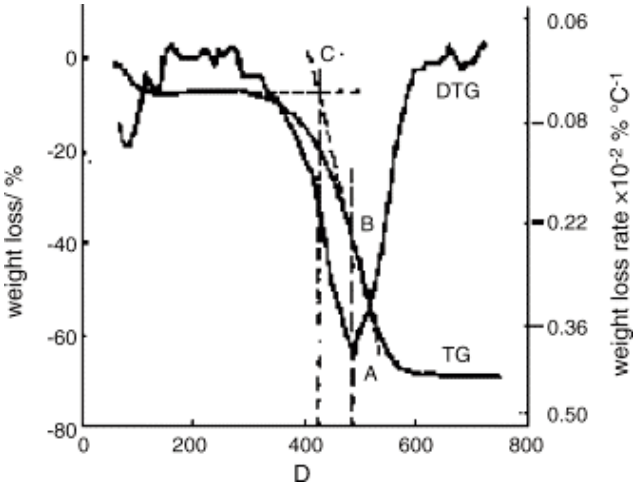

Figure 1: Ignition temperature determination sketch (Nie et al., 2001; Li et al., 2006).

The burnout temperature is defined as the temperature at which there is no noticeable weight loss in the TG and DTG curve.

2.3.3 Ignition index and combustion index

The ignition index D_i and combustion index S were calculated by Equations 11 and 12 according to methods used in previous research involving other biomass samples (El may *et* al., 2009; Vamvuka, 2011; Xiang-guo *et* al., 2006; Sahu *et* al., 2010).

$$D_i = \frac{R_{max}}{t_m t_i} \quad (11)$$

$$S = \frac{R_{max} R_a}{T_i^2 T_b} \quad (12)$$

where R_{max} = maximum combustion rate ($\%°C^{-1}s^{-1}$) being the peak point on the DTG curve in the combustion zone, t_m and t_i = times (s) corresponding to maximum combustion rate and ignition temperature respectively, R_a is the average mass loss rate under oxidative conditions ($\%s^{-1}$), T_i and T_b are ignition and burn-out temperatures (°C) respectively.

3. Results and discussion

3.1 TG and DTG analysis

The TG and the DTG of the samples are presented individually in Figure 2(a)-(d), which must be read together with Figures 3 and 4 to compare the TGs and DTGs of the respective samples. These results show that major thermal decomposition of all the samples followed a similar two stage structural decomposition. The first stage was from: 180 to 355 °C, for PKS (Figure 2a), 200 to 375 °C for ABM wood (Figure 2b), 200 to 350 °C for ABM shell (Figure 2c) and ABT wood (Figure 2d), which is the region of volatile decomposition (oxidative stage). This is the region of cellulose and hemicellulose decomposition. All the samples except PKS experienced greatest mass loss within this stage though at different temperatures due to differences in their structural composition, as can be seen in Table 1. The second stage from 355–500 °C (PKS), 350 – 475 °C (ABM shell), 375–500 °C (ABM wood) and 350–460 °C (ABT wood) region of char combustion.

Figures 2 and 3 show that the decomposition of the biomass samples followed a three step method with the initial mass loss between room temperature and about 110 °C being moisture loss (drying). The amount of moisture lost by each sample is presented in Table 2. There was mass loss observed for PKS and ABM wood between 100 °C and 200 °C before major structural decomposition of the samples. This can be attributed to light volatile release that was not present in other samples.

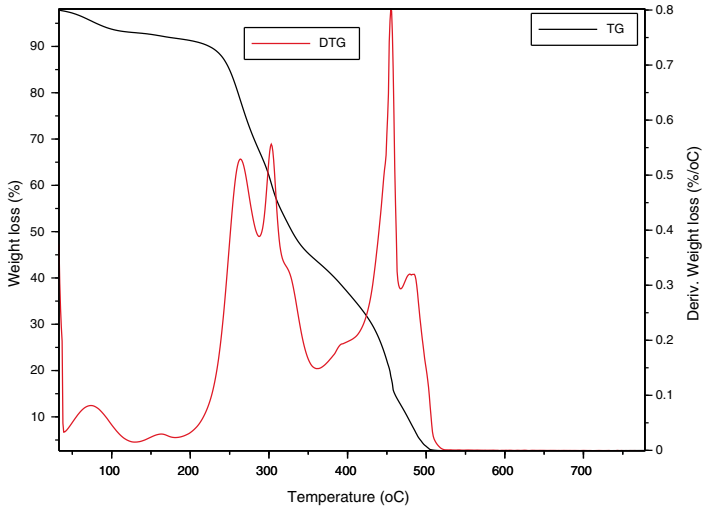

Figure 2a: TG and DTG of Palm kernel shell.

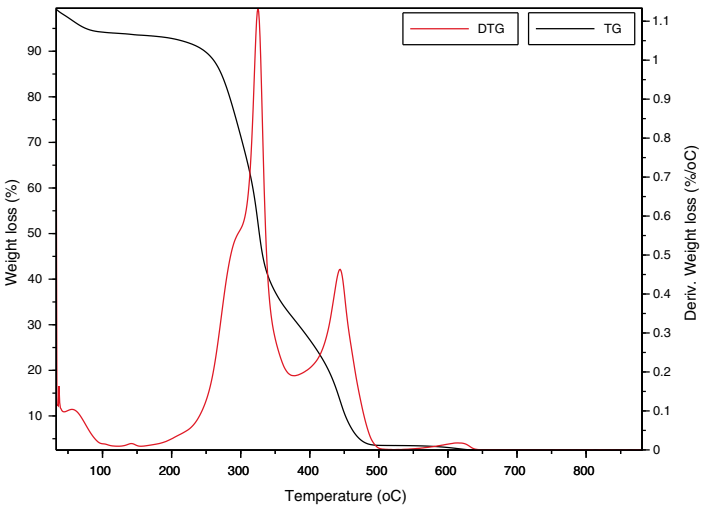

Figure 2b: TG and DTG of African bush mango wood.

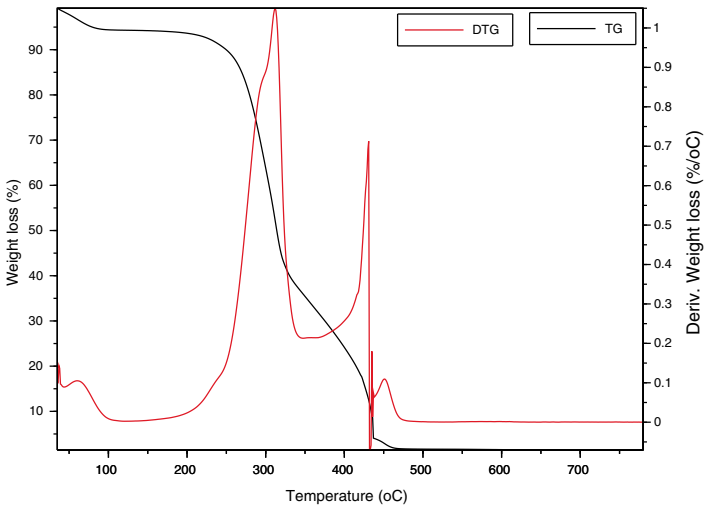

Figure 2c: TG and DTG of African bush mango shell.

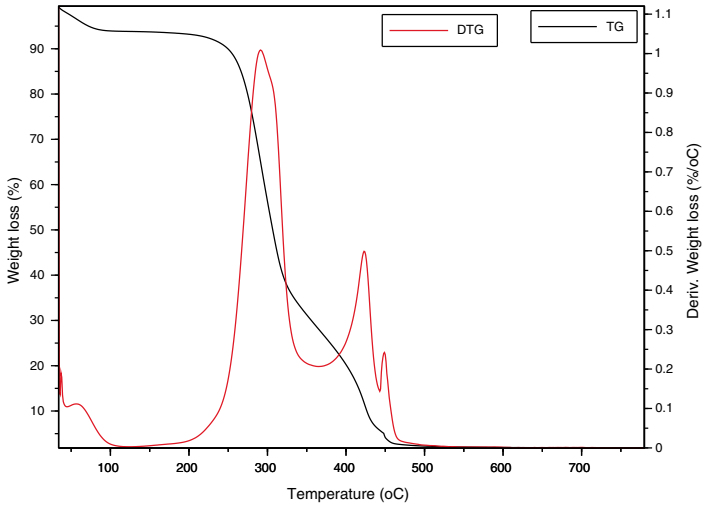

Figure 2d: TG and DTG plot of African border tree wood.

The second and last steps are the decomposition stages, during which the samples reached a complete combustion in the presence of oxygen, decomposing into volatile and ash release respectively. The mass fractions of these products are in Table 2 and Table 3. The TG and DTG profiles show distinctive regions of cellulose and hemicellulose decomposition in the PKS whereas there was no strong indication of this distinctive decomposition of the carbohydrates in the rest of the samples. The hemicellulose decomposition in ABM wood and shell is indicated by the shoulder peak by the left-hand end of their DTG curves while the shoulder peak at the right-hand end of ABT wood DTG shows its cellulose decomposition. The major mass loss in PKS at the combustion zone is confirmed by its large lignin content (Okoroigwe & Saffron, 2012). This is because lignin decomposition takes place over a large range of temperature usually from 180 – 900 °C (Luangkiattikhun, 2008).

3.2 Combustion parameters

3.2.1 Reactivity

The reactivity of the samples in the oxidative and char combustion stages is shown in Tables 2 and 3 respectively. The reactivity index R_M is a measure of

Table 1: Structural carbohydrate and lignin content of samples (Okoroigwe, 2014).

	Lignin (%)	*Cellulose (%)*	*Hemicellulose (%)*	*Inorganic materials (%)*
Palm kernel shell	53.85	6.92	26.16	13.07
African bush mango wood	35.96	40.19	11.47	12.38
African bush mango shell	36.18	36.12	8.77	18.93
African border tree wood	34.96	36.91	18.32	9.81

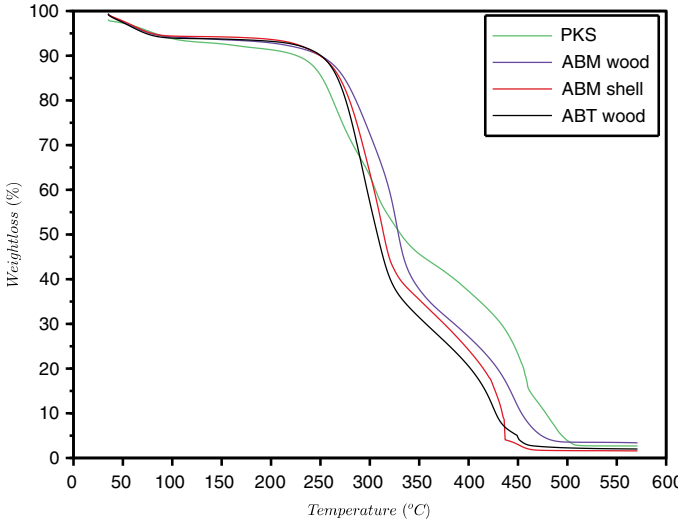

Figure 3: TG of all the samples.

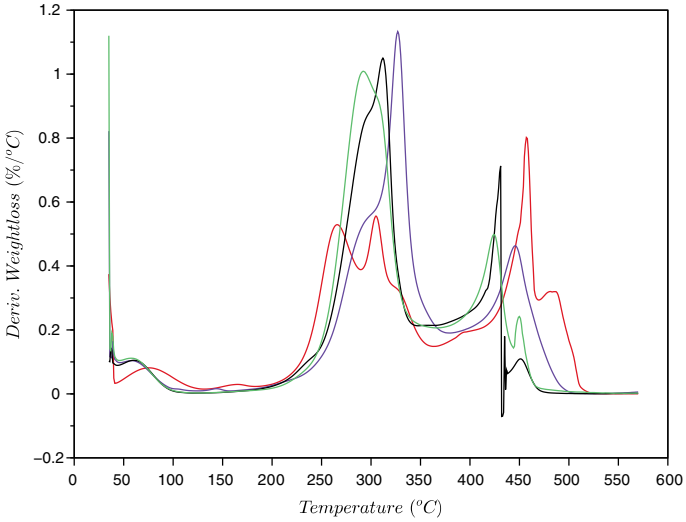

Figure 4: DTG of the samples.

the rate of decomposition of the structural components measured by the peak DTG profiles. The results show that within the volatile decomposition (oxidative) stage, PKS was the least reactive, while ABM shell was the most reactive sample in the mix. This is because the hemicellulose and cellulose components of PKS are small compared to its lignin content (Table 1). On the other hand during the char combustion stage, PKS became the most reactive. These are again expressed by the height of their DTG curves within the regions explained.

3.2.2 Ignition index and combustion index

The ignition and combustion indices of the samples are shown in Table 4, where ABT wood showed the least ignition temperature, T_i, of 275 °C, while PKS showed the highest ignition temperature, T_i, of 293 °C and least ignition index of 1.068 x10^7% °C $^{-1}s^{-2}$. All these could be attributed to the low reactivity of the sample due to its high lignin content. It is not quick to ignite PKS but it releases enormous heat during combustion owing to its high heating value (Okoroigwe & Saffron, 2012). The ABM wood and

Table 2: Combustion parameters during oxidative degradation.

Biomass	*Moisture loss (%)*	*T_{peak} (°C)*	*Volatiles (%)*	*Temperature range (°C)*	*Max. weight loss rate (%°C $^{-1}$)*	*Reactivity R_M x10^3 (%°C $^{-1}s^{-1}$)*	*Av. weight loss rate R_a (%°C $^{-1}$)*
Palm kernel shell	6.0	305	89.0	180 - 355	0.55	0.48	0.2675
African bush mango wood	5.5	325	89.0	200 -375	1.10	0.91	0.3462
African bush mango shell	5.5	315	88.5	200 -350	1.25	1.10	0.3862
African border tree wood	6.0	291	89.0	200 -350	1.01	0.59	0.4098

Table 3: Combustion parameters during char combustion.

Biomass	*Temperature range (°C)*	*T_{peak} (°C)*	*R_{max} (%°C $^{-1}$)*	*Average weight loss rate R_a*	*Reactivity R_M x10^3 (%°C$^{-1}s^{-1}$)*	*Ash (%)*
Palm kernel shell	355–500	455	0.80	0.2822	2.45	5.0
African bush mango wood	375–500	445	0.48	0.2267	0.17	5.5
African bush mango shell	350–475	430	0.71	0.2055	0.29	6.0
African border tree wood	350–460	423	0.49	0.2580	0.20	5.0

Table 4: Combustion characteristics of the samples.								
Sample	T_i (°C)	t_i (s)	R_a (%°C^{-1})	R_{max} (%°C^{-1})	t_{max} (s)	T_b (°C)	$D \times 10^7$ (%°C^{-1}s^{-2})	$S \times 10^9$
Palm kernel shell	293	2300	0.2822	0.8019	3264	500	1.068	5.272
African bush mango wood	290	1648	0.2267	0.4632	2627	495	1.070	2.522
African bush mango shell	285	1672	0.2055	0.7129	2496	475	1.708	3.797
African border tree wood	275	1606	0.2580	0.4986	2489	475	1.247	3.581

its shell have close ignition temperature but have varying ignition index and combustion index. The larger combustion index of the shell might not be unconnected with the larger lignin content than its wood.

3.2.3 Burn-out temperature

Burnout temperature has been applied by researchers to characterise combustion properties of some fuels (Lu & Chen, 2015; Son & Sohn, 2015; Moon et al., 2015). It is defined as a temperature where the rate of weight loss consistently decreases to less than 1%.min^{-1} (Wilson et al., 2011). At this temperature, the sample decomposition can be assumed to be nearly complete and there is no further noticeable mass loss in the form of volatiles. The burnout temperatures, T_b, of the biomass samples used are presented in Table 4. Usually, low burnout temperatures indicate how readily the sample combusts; the lower the burnout temperature, the more readily the fuel is burned (Rostam-Abadi et al., 1988). Among the four samples, ABM shell and ABT wood exhibited the lowest burnout temperature (475 °C) which implies that they can combust more readily than others (Zang et al., 1992; Alvarez & González, 1999) as a result of the samples composition of softer tissues and lower lignin material, as shown in Table 1. Despite the higher content of lignin in ABM shell than the ABM wood, as shown in Table 1, its burning was aided by the oil content of the kernel (housed in the shell). The burnout temperatures were, however, higher than 377, 365, 364, 378 and 382 °C obtained by Wilson et al. (2011), for mill bagasse, palm stem, cashew nut shells, coffee husks and sisal bole biomass species found in the tropics. In spite of these being all tropical plants, two different biomass samples are most likely to differ in their thermal characteristic behaviour due to agronomical differences. The burnout temperature results reported in this investigation can be attributed to the morphological and agronomical differences of the samples used. It can,

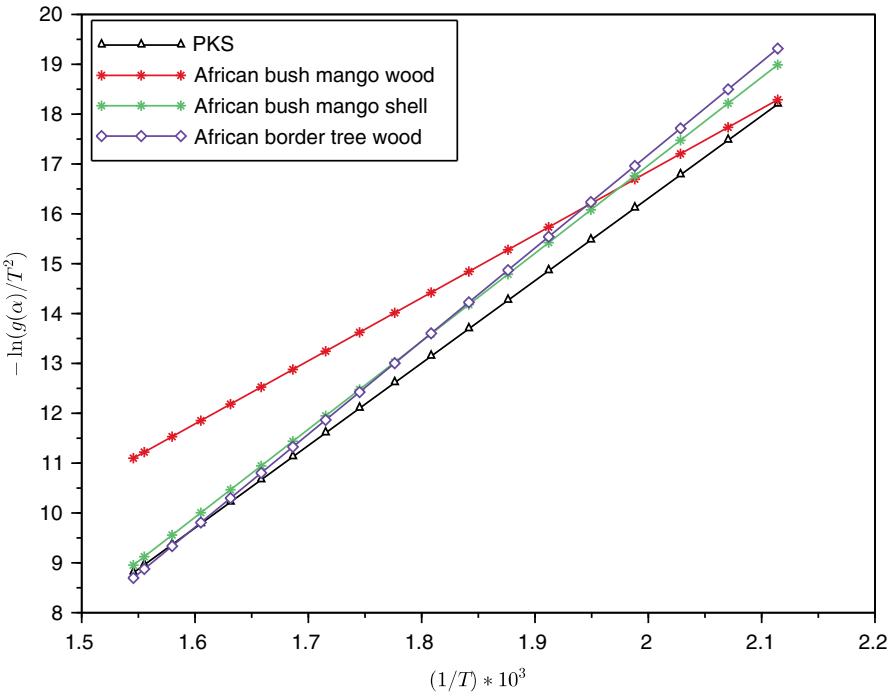

Figure 5a: Plots of $\left[\frac{g(\alpha)}{T^2}\right]$ against T^{-1} for all samples during oxidative stage.

therefore, be inferred that the mill bagasse, palm stem, cashew nut shells, coffee husks and Sisal bole are more readily combustible than the current samples being studied.

3.3 Kinetic parameters

The plot of logarithmic rate of reaction $\left[\frac{g(a)}{T^2}\right]$ against reciprocal of temperature, T^{-1}, (Equation 9) for all the samples during oxidative and char combustion stages is shown in Figure 5 and the summary of the parameters estimated using the intercept and slope of each sample's plot for the two stages are presented in Tables 5 and 6.

The activation energy of any sample undergoing chemical reaction is usually the threshold energy the particles would overcome before the reaction can proceed (White et al., 2011). Applied here, activation energy is the minimum energy required to start the decomposition reaction.

As observed from Tables 5 and 6, the activation energy of each sample varied as reaction moved from volatile decomposition stage to char combustion stage. Volatile decomposition is a low-temperature reaction relative to a high-temperature combustion reaction, hence the lower energy requirement at the oxidation stage. Comparison of the activation energy of the samples shows that ABM wood had the lowest activation energy, of 99.03 $kJ.mol^{-1}$, while ABT wood had the highest activation energy, of 124.35 $kJ.mol^{-1}$. During the combustion stage PKS had the lowest value, of 155.62 $kJ.mol^{-1}$, while ABM shell experienced the highest value, of 403.78 $kJ.mol^{-1}$. The two-stage structural decomposition process showed that the activation energy values were proportional to the process reaction order and the same for frequency factors. There is limited literature on the activation energy of the current samples, except for PKS, whose activation energy is within the range reported by Idris et al. (2012) despite using different experimental methods by them. The activation energy of the four samples were compared with those of other biomass samples reported (Wilson et al., 2011; Shen et al., 2009), as presented in Table 7.

Table 7 shows that the average activation energy values of current samples differ from those reported by other researchers for different biomass samples at different heating rates. Heating rate, particle size, model employed in the analyses, and the experimental medium are among the factors that can affect the combustion parameter estimation. Insufficient and/or lack of research in the reactivity behaviour of samples similar to the current ones and perhaps their heterogeneous nature, might be responsible for the differences in comparison with others. The values obtained in this investigation can, therefore, be accepted in the context of the associated experiment and can be used to predict the combustion behaviour of the feedstock. Generally, however, the values obtained here are lower than those reported by Wilson et al. (2011) for palm stem, cashew nut shells, coffee husks and sisal bole, even though they differ in morphology and plant family. They are also higher than those of oak, aspen, birch and pine reported by Shen et al. (2009). The implication is that less energy is required to convert the samples in this work to bioenergy than the samples reported by Wilson et

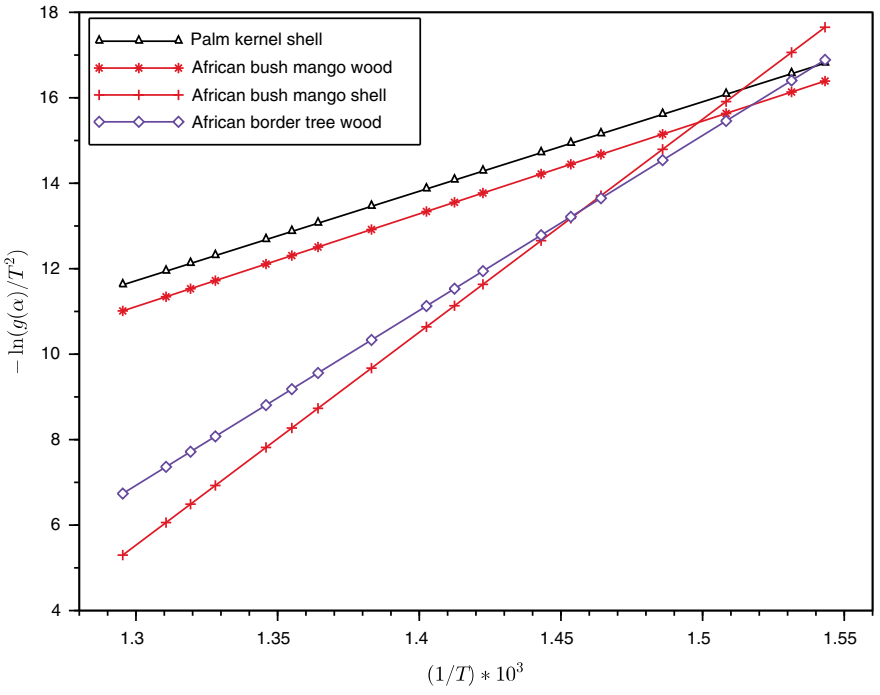

Figure 5b: Plots of $\left[\frac{g(\alpha)}{T^2}\right]$ against T^{-1} for all samples during char combustion stage.

Table 5: Summary of the estimated kinetic reaction parameters representing the volatile decomposition stage.

Sample	***Reaction order, n***				***Reaction kinetic parameters***		
	Factor of correlation, R^2				*Determined reaction order*	*Activation energy, E*	*Frequency factor, A*
	0	*1*	*2*	*3*	*n*	*(kJ.mol^{-1})*	*(min^{-1})*
Palm kernel shell	0.8291521	0.9331554	0.9780643	0.9516838	2	124.35042	11926.583
African bush mango wood	0.9406571	0.9852757	0.9659244	0.9002804	1	99.035323	7124.4312
African bush mango shell	0.9118338	0.9732715	0.9847963	0.9453636	2	135.50204	13644.02
African border tree wood	0.895209	0.9628088	0.989191	0.961295	2	144.3738	15141.96

Table 6: Summary of the estimated kinetic reaction parameters representing the char combustion stage.

Sample	***Reaction order, n***				***Reaction kinetic parameters***		
	Factor of correlation, R^2				*Determined reaction order*	*Activation energy, E*	*Frequency factor, A*
	0	*1*	*2*	*3*	*n*	*(kJ.mol^{-1})*	*(min^{-1})*
Palm kernel shell	0.8722524	0.9553034	0.9359161	0.868101	1	155.62467	14301.637
African bush mango wood	0.8145269	0.9657425	0.9140365	0.836295	1	163.90929	15925.278
African bush mango shell	0.7673127	0.9587005	0.9658252	0.926689	2	403.78535	59633.139
African border tree wood	0.6956617	0.9252994	0.9846007	0.955613	2	318.29011	43503.998

Table 7: Comparison of average activation energy of the samples with those of other biomass samples.

Sample	***Activation energy (kJ.mol^{-1})***	***Heating rate (k.min^{-1})***	***Particle size used (mm)***	***Reference***
Palm kernel shell	139.988	30	1	Current
African bush mango wood	131.472	-30	1	Current
African bush mango shell	269.643	30	1	Current
African border tree wood	231.332	30	1	Current
Mill bagasse	460.60	10	Not given	Wilson et al., 2011
Palm stem	542.07	10	Not given	Wilson et al., 2011
Cashew nut shells	293.48	10	Not given	Wilson et al., 2011
Oak	104–125	10–100	<0.5	Shen et al., 2009
Aspen	104–125	10–100	<0.5	Shen et al., 2009
Pine	104–125	10–100	<0.5	Shen et al., 2009
Birch	104–125	10–100	<0.5	Shen et al., 2009

al., but may require more energy than those reported by Shen et al. In addition to using different samples from the ones reported by Wilson et al. and Shen et al., geographical location, climatic conditions and biomass origin can contribute to the variation in the parameters obtained.

4. Conclusions

The combustion characteristics and decomposition kinetics of the biomass samples under oxidative conditions were studied. The thermal decomposition process showed distinctly the regions of moisture loss, structural decomposition and char combustion stages.

At the heating rate of 30 °C.min^{-1} the volatile release stage was the most critical of the degradation process in all the samples because the greater mass loss was observed in this region, with the exception only of PKS. The greater combustion process of the samples, except for PKS, would, therefore, most likely take place at this temperature region, with lower degree of combustion taking place at the higher temperatures.

The samples were characterised by low activation energies and decomposed at low energy input compared with some biomass samples reported in literature under combustion conditions but different heating rate and particle size. The samples also displayed high reaction rates during the structural decomposition stages with high volatile release.

Under an oxygenated medium, the combustion processes of the samples was complete, leading to low-carbon emission, which is a good attribute of biomass combustion for bioenergy production.

Owing to lack of reports on oxidative and combustion characteristics of the biomass samples studied in this research, further investigation involving varying particle size, heating rates, pre-treatments, cultivation, location and biomass age (maturity) are proposed. This will not only provide additional information on the combustion properties of the samples but also validate the results presented in this research.

References

Ainge L. and Brown, N. Irvingia genensis and wombolu: a state of knowledge report undertaken for the Central African Regional program for the environment. Oxford Forestry Institute, Department of Plant Sciences, University of Oxford United Kingdom, 2001. Online: http://carpe.umd.edu/Documents/2001/report-ainge-brown2001.pdf (accessed 23/3/2015).

Alvarez, E. and González, J. F. 1999. Combustion of Spanish coals under simulated pressurized–fluidized-bed-combustion conditions. *Fuel* 78: 335–340.

Anyaoku, O. A. 2007. Nigerian bio-fuel policy and incentives, *Official gazette of the Nigerian bio-fuel policy and incentives, Federal Republic of Nigeria*. Online: www.sunbirdbioenergy.com/docs/Nigeria_E10_POLICY_GAZETTED.pdf

Apaydin-Varol, E. Polat, S. and Putun, A. E. 2014. Pyrolysis kinetics and thermal decomposition behaviour of polycarbonate – a TGA-FTIR study. *Thermal Science* 18(3): 833 – 842.

Ayuka, E. T., Duguma, B., Franzel, S., Kengue, J., Mollet, M., Tiki-Manga, T. and Zenkeng, P. 1999. Uses, management and economic potential of Irvingia gabonensis in the humid lowlands of Cameroon. *Forest Ecology and Management* 113(1): 1–9.

Bafor, E. and Sanni, U. 2009. Uterine contractile effects of the aqueous and ethanol leaf extracts of newbouldia laevis (Bignoniaceae) in vitro. *Indian Journal of Pharmaceutical Science*, 2009, 71(2):124–127.

Coats, A. W. and Redfern, J. P. 1964. Kinetic parameters from thermogravimetric data. *Nature* 201:68–69.

Conesa, J.A. and Rey, L. 2015. Thermogravimetric and kinetic analysis of the decomposition of solid recovered fuel from municipal solid waste, *Journal of Thermal Analysis and Calorimetry.* 120: 1233–1240. doi 10.1007/s10973-015-4396-4.

Department of Minerals and Energy. 2007. *Biofuels industrial strategy of the Republic of South Africa*, Online: www.energy.gov.za/files/esources/renewables/biofuels_indus_strat.pdf%282%29.pdf (accessed 09/02/2015).

Ejele, A.E., Enenebaku, C.K., Akujobi, C.O. and Ngwu, S.U. 2012. Effect of microbial spoilage on phytochemistry, antisickling and antimicrobial potential of Newbouldia laevis leaf extract, *International Research Journal of Microbiology* 3(4):113-116.

El may, Y., Mejdi, J., Sophie D., Gwenaelle, T, and Rachid, S. 2012. Study on the thermal behaviour of different date palm residues: characterization and devolatilization kinetics under inert and oxidative atmospheres. *Energy* 44: 702–709. http://dx.doi.org/10.1016/j.energy.2012.05.022.

Extension Bulletin. 1999. Production and utilization of 'ogbono, African bush mango' (Irvingia gabonensis), *Extension Bulletin no 140, Horticulture Series no 4*. National Agricultural Extension and Research Liaison Services, Federal Ministry of Agriculture and Water Resources, ABU Zaria.

Ghetti, P., Leandro, R. and Luciana, A. 1966. Thermal analysis of biomass and corresponding pyrolysis products. *Fuel* 75(5):565 – 573.

Idris, S. S., Rahman, N. A. and Ismail, K. 2012. Combustion characteristics of Malaysian oil palm biomass, sub-bituminous coal and their respective blends via thermogravimetric analysis (TGA). *Bioresource Technology* 123:581–591.

Jeguirim, M., Bikai, J., El may, Y., Limousy, L., and Njeugna, E. 2014. Thermal characterization and pyrolysis kinetics of tropical biomass feedstocks for energy recovery. *Energy for Sustainable Development* 23:188–193.

Lin, R., Zhu, Y. and Tavlarides, L.L. 2013. Mechanism and kinetics of thermal decomposition of biodiesel fuel. *Fuel* 106:593–604.

Lu, J-J. and Chen, W-H. 2015. Investigation on the ignition and burnout temperatures of bamboo and

sugarcane bagasse by thermogravimetric analysis. *Applied Energy* 160:49–57.

Luangkiattikhun, P., Tangsathitkulchai, C. and Tangsathitkulchai, M. 2008. Non-isothermal thermogravimetric analysis of oil-palm solid wastes. *Bioresource Technology* 99:986– 997.

Moon, C., Sung, Y., Eom, S. and Choi G. 2015. NOx emissions and burnout characteristics of bituminous coal, lignite, and their blends in a pulverized coal-fired furnace. *Experimental Thermal and Fluid Science* 62:99–108.

Munir, S., Daood, S. S., Nimmo, W., Cunliffe, A. M. and Gibbs, B. M. 2009. Thermal analysis and devolatilization kinetics of cotton stalk, sugar cane bagasse and shea meal under nitrogen and air atmospheres. *Bioresource Technology* 100:1413-1418.

Ninan, K. N. 1989. Kinetics of solid-state thermal decomposition reactions, *Journal of Thermal Analysis* 35:1267–1278.

Niu, Z., Liu, G., Yin, H., Wu, D. and Zhou, C. 2016. Investigation of mechanism and kinetics of non-isothermal low temperature pyrolysis of perhydrous bituminous coal by in-situ FTIR. *Fuel* 172:1–10.

Okoroigwe, E. C. Energy conversion of woody biomass by fast pyrolysis method. 2014. PhD dissertation. University of Nigeria, Nsukka, Nigeria.

Okoroigwe, E. C. and Saffron, C. M. 2012. Determination of bio-energy potential of palm kernel shell by physicochemical characterization. *Nigerian Journal of Technology*. 31(3): 329–335.

Okpala, B. 2015. Incredible benefits of newbouldia laevis (ogilisi). *Global food book.* Online: http://global-foodbook.com/incredible-benefits-of-newbouldia-laevis-ogilisi/.

Park, S. W. and Jang, C. H. 2012. Effects of pyrolysis temperature on changes in fuel characteristics of biomass char. *Energy* 39:187 – 195.

Parthasarathy, P. Narayanan, K. S. and Arockiam, L. 2013. Study on kinetic parameters of different biomass samples using thermo-gravimetric analysis. *Biomass and Bioenergy* 58:58–66.

Rainville, E. D. 1960. *Special Functions*. New York: Macmillan.

Roberts, M. J., Everson, R. C., Domazetis, G, Neomagus, H.W.J.P., Jones, J.M., Van Sittert, C.G.C.E., Okolo, G.N., Van Niekerk, D. and Mathews, J. P. 2015. Density functional theory molecular modelling and experimental particle kinetics for CO_2–char gasification. *Carbon* 93:295–314.

Rostam-Abadi, M., DeBarr, J. A. and Moran, D. L. 1988. Burning characteristics of partially devolatilized coals. *Fuel Chemistry*33:869-874.

Sahu, S. G., Sarkar, P., Chakraborty, N. and Adak, A. K. 2010. Thermogravimetric assessment of combustion characteristics of blends of a coal with different biomass chars. *Fuel Processing Technology* 91(3):369–378.

Shen, D. K., Gu, S., Luo, K. H., Bridgwater, A. V., and Fang, M. X. 2009. Kinetic study on thermal decomposition of woods in oxidative environment. *Fuel* 88:1024–1030.

Soccol, C. R., Vandenberghe, L. P. S., Costa, B., Woiciechowski, A. L., De Carvalho, J. C., Medeiros A. B. P., Franscisco, A. M. and Bonomi, L. J. 2005. Brazilian biofuel program: An overview. *Journal of Scientic and Industrial Research* 64(11):897–904.

Son, J. W. and Sohn, C. H. 2015. Evaluation of burnout performance of biomass wastes in a rocket-engine-based incinerator. *Fuel* 143:308–317.

União Brasileira do Biodiesel e Bioquerosene (Ubrabio) and Getulio Vargas Foundation. 2010. Biodiesel and its contribution to Brazilian development, 1-34. Online: http://fgvenergia.fgv.br/sites/fgvenergia.fgv.br/files/ubrabio.pdf

Vamvuka, D. and Sfakiotakis, S. 2011. Combustion behaviour of biomass fuels and their blends with lignite. *Thermochimica Acta* 526:192–199.

Wilson, L., Yang, W., Blasiak, W., John, G. R.and Mhilu, C. F. 2011. Thermal characterization of tropical biomass feedstocks, *Energy Conversion and Management* 52:191–198.

Xiang-guo, L., Bao-guo, M., Li, X., Zhen-wu, H. and Xin-gang, W. 2006. Thermogravimetric analysis of the co-combustion of the blends with high ash coal and waste tyres. *Thermochimica Acta* 441:79–83.

Zhang, D., Wall, T.F., and Tate, A.G. 1992. The reactivity of pulverized coal char particles; experiments using ignition, burnout and DTG techniques and partly burnt chars. *Fuel* 71:1247–1253.